

Article

CO₂ Monitoring and Background Mole Fraction at Zhongshan Station, Antarctica

Yulong Sun ^{1,3}, Lingen Bian ^{1,2,*}, Jie Tang ², Zhiqiu Gao ³, Changgui Lu ²
and Russell C. Schnell ⁴

¹ Climate and Weather Disasters Collaborative Innovation Center, Nanjing University of Information Science & Technology, Nanjing 210044, China; E-Mail: sunyulong211@gmail.com

² Chinese Academy of Meteorological Sciences, Beijing 100081, China;
E-Mails: tangj@cams.cma.gov.cn (J.T.); lcg@cams.cma.gov.cn (C.L.)

³ College of Applied Meteorology, Nanjing University of Information Science & Technology, Nanjing 210044, China; E-Mail: zgao@nuist.edu.cn

⁴ NOAA ESRL Global Monitoring Division, 325 Broadway, R/GMD, Boulder, CO 80305, USA; E-Mail: Russell.C.Schnell@noaa.gov

* Author to whom correspondence should be addressed; E-Mail: blg@cams.cma.gov.cn;
Tel.: +86-10-6840-6566; Fax: +86-10-6217-5931.

Received: 8 July 2014; in revised form: 12 September 2014 / Accepted: 15 September 2014 /

Published: 24 September 2014

Abstract: Background CO₂ mole fraction and seasonal variations, measured at Zhongshan station, Antarctica, for 2010 through 2013, exhibit the expected lowest mole fraction in March with a peak in November. Irrespective of wind direction, the mole fraction of CO₂ distributes evenly after polluted air from station operations is removed from the data sets. The daily range of average CO₂ mole fraction in all four seasons is small. The monthly mean CO₂ mole fraction at Zhongshan station is similar to that of other stations in Antarctica, with seasonal CO₂ amplitudes in the order of 384–392 μmol·mol⁻¹. The annual increase in recent years is about 2 μmol·mol⁻¹·yr⁻¹. There is no appreciable difference between CO₂ mole fractions around the coast of Antarctica and in the interior, showing that CO₂ observed in Antarctica has been fully mixed in the atmosphere as it moves from the north through the southern hemisphere.

Keywords: Antarctica; Zhongshan Station; CO₂; background; CO₂ characteristics

1. Introduction

CO₂ is a greenhouse gas with a long life span (hundreds of years) that absorbs infrared radiation in the 12 μm to 17 μm waveband and contributes ~60% global of the greenhouse gas warming potential in the atmosphere [1–3]. Since the industrial revolution, the mole fraction of CO₂ has been rising and has accelerated in recent years, reaching 400 μmol·mol⁻¹ at Mauna Loa Observatory, Hawaii, in March 2014, up from 275 μmol·mol⁻¹ prior to the industrial revolution [4–7]. The continuous increase in the mole fraction of all greenhouse gases has elevated atmospheric radiative forcing (climate warming potential) by 34% from 1990 to 2013 [8–12].

This increase is mainly caused by human activities and has attracted the attention of governments and the scientific community around the world [13,14]. Far away from major combustion sources that are the main drivers of increasing global atmospheric CO₂ mole fraction, Antarctica is an ideal area for observing the background levels of greenhouse gases in the global atmosphere [15]. Through flask sampling of air collected at the South Pole station, and later lab analysis in California, Keeling *et al.* [16] pointed out that the mole fraction of CO₂ in the Antarctic atmosphere increased by 3.7% from 1957 through 1971, at an average annual increase of 1.3 μmol·mol⁻¹·yr⁻¹, from 315 μmol·mol⁻¹ in 1958 to 380 μmol·mol⁻¹ in 2007 [17]. Morimoto *et al.* [18] indicated that the mole fraction of CO₂ at Syowa station increased from 342 μmol·mol⁻¹ in 1984 to 368 μmol·mol⁻¹ in 2000, with an average annual increase of 1.49 μmol·mol⁻¹·yr⁻¹. Ghude *et al.* [19] observed that around the Antarctic Circle, over the past 22 years, the increase in the rate of CO₂ mole fraction from 1992 through 2004 is 1.2 times faster than that during 1983 through 1991.

Flask sampling and lab analyses have a long history in the monitoring of greenhouse gases at Antarctic stations. As such, flask sampling frequency is usually once a week. With the support of the 4th International Polar Year (2008/2009) China Action Plan, continuous CO₂ monitoring was instituted at Zhongshan Station, Antarctica, by the 24th Antarctic expedition team. In this paper, an analysis of CO₂ mole fractions, measured continuously from 2010 through 2013, along with associated surface meteorological observations at Zhongshan Station, are presented and discussed.

2. Observation Point and Monitoring Instruments

2.1. Site Location

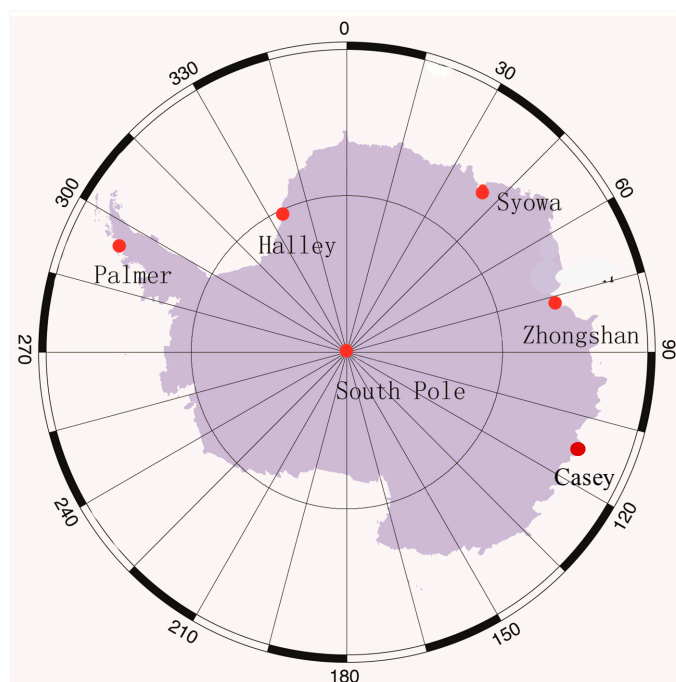
Zhongshan Station is located on the east coast of Antarctica (Figure 1). Influences from generating electricity in the main station area, transportation patterns, and other human activities were taken into consideration in selecting the site as the CO₂ observation point [20], which is built on an outcropping rock in the Tian'e Range, northwest of the station (69°22'2''S, 76°21'49''E, 18.5 m). At this site east-northeast winds prevail all year round.

2.2. Instrumentation

A high-precision CO₂/CH₄/H₂O analyzer (Model G1301, by Picarro, Santa Clara, California, USA) is used in the measurement of CO₂ and CH₄ at the Zhongshan station [21]. The instrument has a temperature and pressure control systems that maintains good linearity and accuracy when the

surrounding environmental conditions change. The air inlet tubing constructed of 3/8"OD Syflex 1300 is set on the roof of the cabin at a height of 5 m above ground. Aerosol particles in the sample stream are removed with a 7 μm filter before the gas enters a KNF transfer pump. The output pressure release controller is set at 103.4 kPa (15 psi). A small secondary pressure release valve is installed behind the glass cold trap pipe to ensure to reduce the influence of air enrichment. To stabilize the air flow, a high-precision flow controller was installed before the air entering the analyzing system [22].

Figure 1. The location of other CO₂ monitoring stations in Antarctica relative to Zhongshan station.

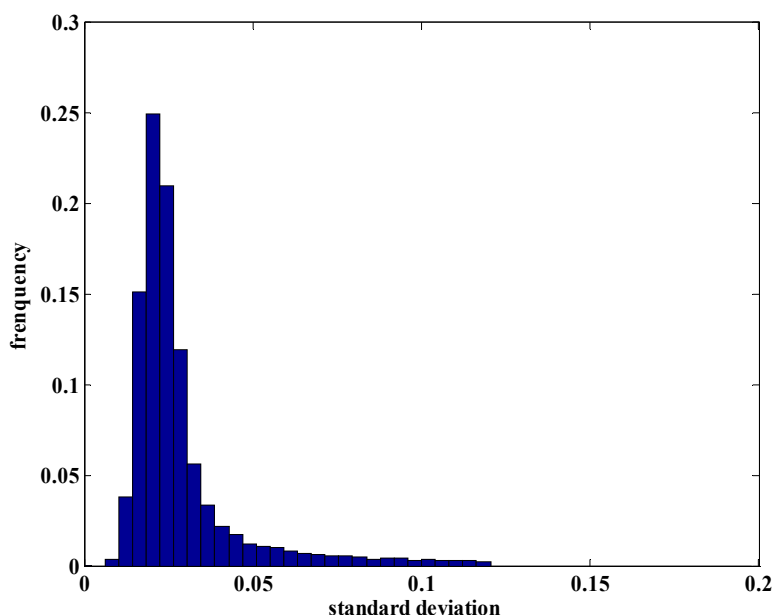


The Picarro CO₂/CH₄/H₂O analyzer was installed in an isolated cabin along with reference gas tanks calibrated at NOAA/ESRL on the WMO standard scale with CO₂ and CH₄ mole fractions close to ambient. On site, as station standard gases, three cylinders of reference gases purchased from NOAA/GMD, are used to calibrate the instrument once every three months. Two compressed air cylinders are used as target gases to check the instrument drift twice per day [23]. The 5 min standard deviation of target gases measurements are from 0.013 $\mu\text{mol}\cdot\text{mol}^{-1}$ (5% percentile) to 0.052 $\mu\text{mol}\cdot\text{mol}^{-1}$ (95% percentile). The instrument drifts confirmed with the calibration data and the target gases measurement are less than 0.08 $\mu\text{mol}\cdot\text{mol}^{-1}$ per year. The analyzer pulled air from the inlet continuously at 300 sccm (standard cubic centimeters per minute) and measured at 0.5 Hz. The CO₂ and CH₄ data were corrected for water vapor using a correction that was determined using the same analyzer unit. For CO₂ this calibration is consistent with the manufacturer's correction within 0.1 $\mu\text{mol}\cdot\text{mol}^{-1}$ (Picarro does not provide a correction for CH₄). The correction is also consistent to within 0.1 $\mu\text{mol}\cdot\text{mol}^{-1}$ for CO₂ and 1 $\text{nmol}\cdot\text{mol}^{-1}$ for CH₄ with that found by another group testing the same analyzer [24]. The analysis time is 2 s per measurement with a precision of $\pm 0.05 \mu\text{mol}\cdot\text{mol}^{-1}$ for CO₂ and $\pm 1 \text{ nmol}\cdot\text{mol}^{-1}$ for CH₄, meeting the requirements of WMO-GAW for gas analysis, calibration and classification [25].

3. Data Processing

Before processing the raw data, periods of zero gas, short-time power failures and equipment maintenance were deleted. Then the daily check value and the calibration data obtained every three months were used to correct the raw data. The hourly standard deviations of CO₂ mole fraction, thus obtained, are shown in Figure 2. As seen in this figure, the distribution of the standard deviation is extremely sharp. We first rejected the hourly means with standard deviations of more than 0.1 $\mu\text{mol}\cdot\text{mol}^{-1}$ within an hour. Abnormal values were then removed on the basis of the formula $|x_i - \bar{x}| > 3\sigma$, where x_i is measured value, \bar{x} is the mean value and σ is the standard deviation of the hourly means. After processing, 92% of the hourly mean data was retained.

Figure 2. Distribution of hourly standard deviations of CO₂ mole fraction observed at Zhongshan Station for the period of 2010–2013.



This processing cannot completely exclude the impact of emissions from the station area. Wind is an important factor that causes fluctuations in observation [26,27]. Ten meter wind data at Zhongshan station was used to work out the frequency, corresponding average speed and CO₂ mole fraction in 16 directions. Figure 3 presents the Wind Frequency (WF), average Wind Speed (WS), and average CO₂ mole fraction under each wind direction category during 2010 through 2013. From this figure, it can be observed that the prevailing winds are persistent easterly winds with 83.1%, coming from the quadrant in the ENE, E and ESE. This indicates that the observation sampling point is located well in the direction of upstream airflow. This airflow mainly comes from the Antarctic continent sea ice cover and easterly sea areas. The mole fraction of CO₂ under easterly winds is 388.8 $\mu\text{mol}\cdot\text{mol}^{-1}$, whereas, for westerly winds it is relatively higher at 389.3 $\mu\text{mol}\cdot\text{mol}^{-1}$, followed by north (389.2 $\mu\text{mol}\cdot\text{mol}^{-1}$) and south winds (389.1 $\mu\text{mol}\cdot\text{mol}^{-1}$), respectively. Mole fractions in winds from other directions are within the range of 388.9–389.1 $\mu\text{mol}\cdot\text{mol}^{-1}$. On the whole, the wind direction does not influence the CO₂ mole fraction significantly.

Figure 3. Wind Frequency, Wind Speed and CO₂ mole fractions under 16 wind directions (2010 through 2013). Scale 10–50 is used for WF and WS and Scale 386–390 for CO₂.

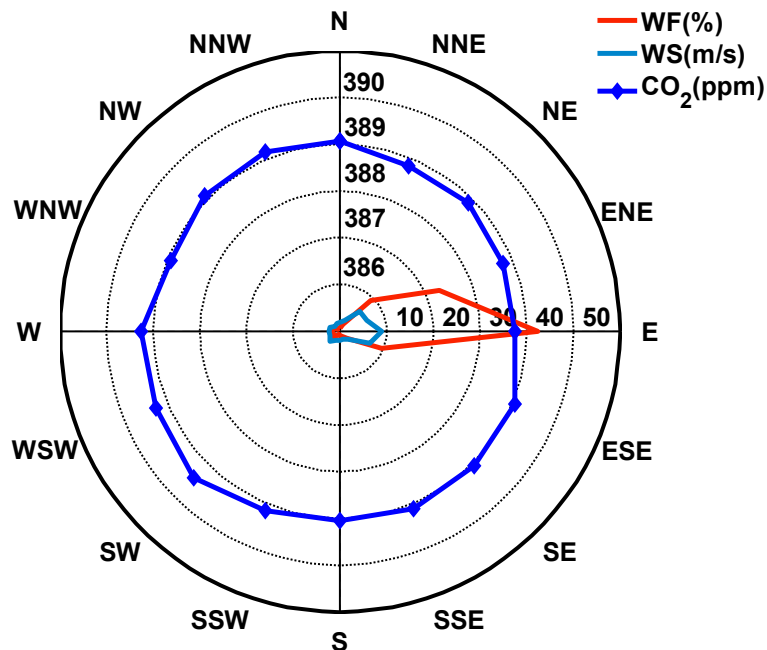


Figure 3 displays the WF, WS and CO₂ mole fraction under different wind directions in Spring (September–November), Summer (December–February.), Autumn (March–May), and Winter (June–August) during 2010 through 2013. From Figure 4 it may be observed that there is little difference between the prevailing wind directions in the four seasons: only the frequency of NE winds increases in spring and summer. The distribution of wind speed in each season differs insignificantly from that throughout the year: the maximum wind speed appears under easterly winds of which frequency is also the highest. CO₂ mole fractions are similar to each other under different wind directions, although in winds from the S-SSW the CO₂ mole fraction rises in spring and reduces in summer. That may be somewhat influenced by the relatively limited samples in this wind direction. Under easterly winds, CO₂ mole fractions in autumn go down slightly probably signifying the influx of northern hemisphere air or depletions of CO₂ by the growth of marine plankton.

Slow and variable direction winds are not conducive to the diffusion and mixing of pollutants. As such, wind speed data from 2010 through 2013 were divided into seven groups as follow: $\leq 0.5 \text{ m}\cdot\text{s}^{-1}$, $0.5\text{--}3 \text{ m}\cdot\text{s}^{-1}$, $3\text{--}6 \text{ m}\cdot\text{s}^{-1}$, $6\text{--}10 \text{ m}\cdot\text{s}^{-1}$, $10\text{--}15 \text{ m}\cdot\text{s}^{-1}$, $15\text{--}20 \text{ m}\cdot\text{s}^{-1}$, and $>20 \text{ m}\cdot\text{s}^{-1}$. Figure 5 displays the CO₂ mole fraction in each wind speed scale, where it may be observed that 94.7% of winds fall in the $0.5 \text{ m}\cdot\text{s}^{-1}$ to $15 \text{ m}\cdot\text{s}^{-1}$ range with only 1% of winds above $20 \text{ m}\cdot\text{s}^{-1}$. The wind can be classified as calm at $\leq 0.5 \text{ m}\cdot\text{s}^{-1}$ of which frequency of occurrence is 0.3% when the CO₂ mole fraction is slightly elevated. In order to keep the background CO₂ mole fraction data free from possible contaminated values, the data during calm wind condition has been removed from CO₂ mole fraction analyses.

The frequency of each wind speed scale in four seasons, and the respective change in CO₂ mole fractions, are shown in Figure 6. In autumn and winter, when the wind speed is $\leq 0.5 \text{ m}\cdot\text{s}^{-1}$, CO₂ mole fractions are unstable, which is probably caused by local influence from the station area. In spring and summer, under similar wind conditions, the CO₂ mole fraction changes little. This indicates that although the CO₂ observation point is only 500 m away from the station, wind speed exerts a relatively small

influence on the observed CO₂ mole fractions since the total emissions from the station are limited. After the processing and analysis above, 1.7% of the data was removed. Thus, the processed data may be used to represent the background CO₂ mole fractions in the region.

Figure 4. WF, WS, and CO₂ mole fraction under 16 wind directions in four seasons. Scale 10–50 is used for WF and WS and Scale 386–390 for CO₂.

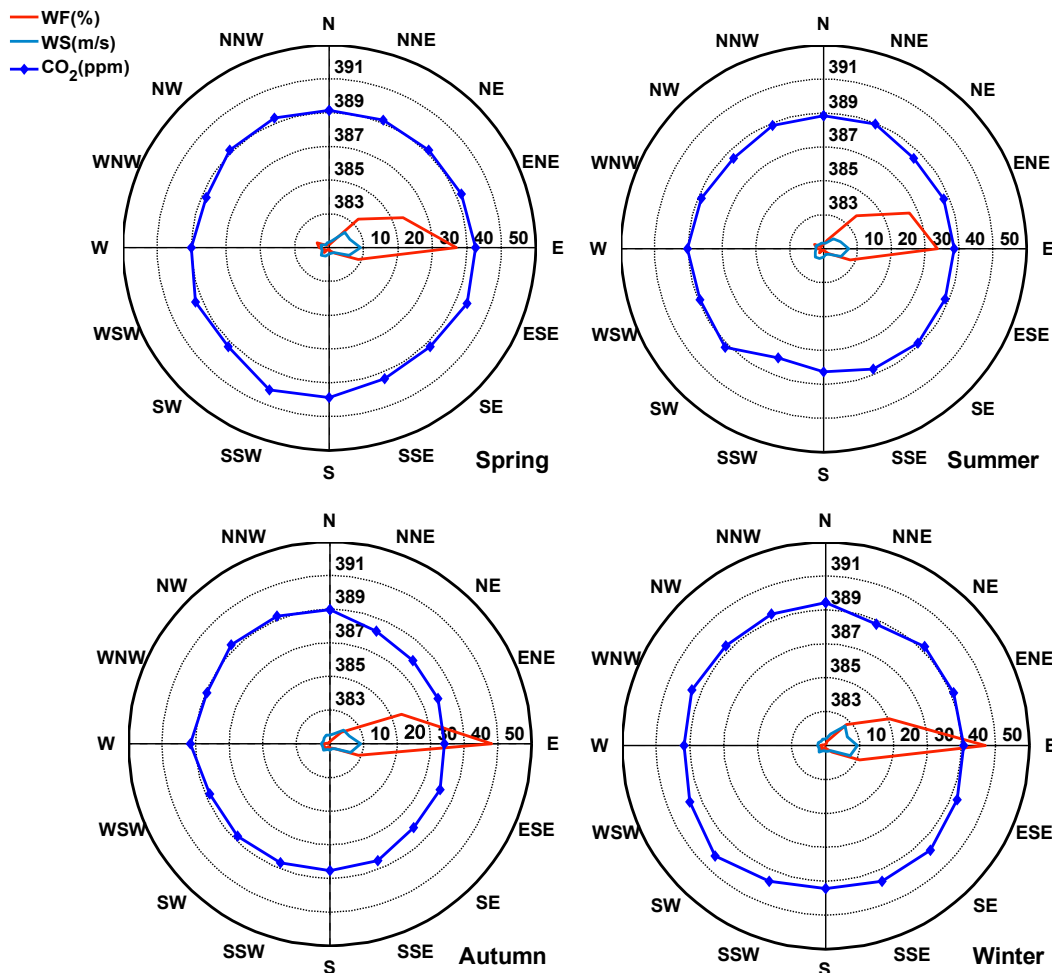


Figure 5. Frequency of occurrence of different wind speed scale and corresponding CO₂ mole fraction (2010 through 2013). The black bars stand for frequency of occurrence. The vertical bars stand for the amplitude of CO₂ mole fractions under the condition of same wind speed scale.

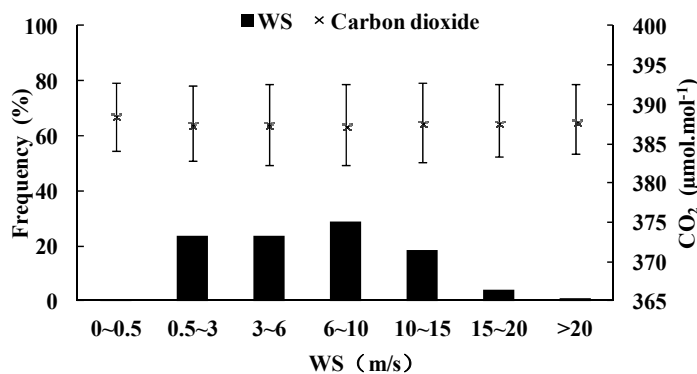
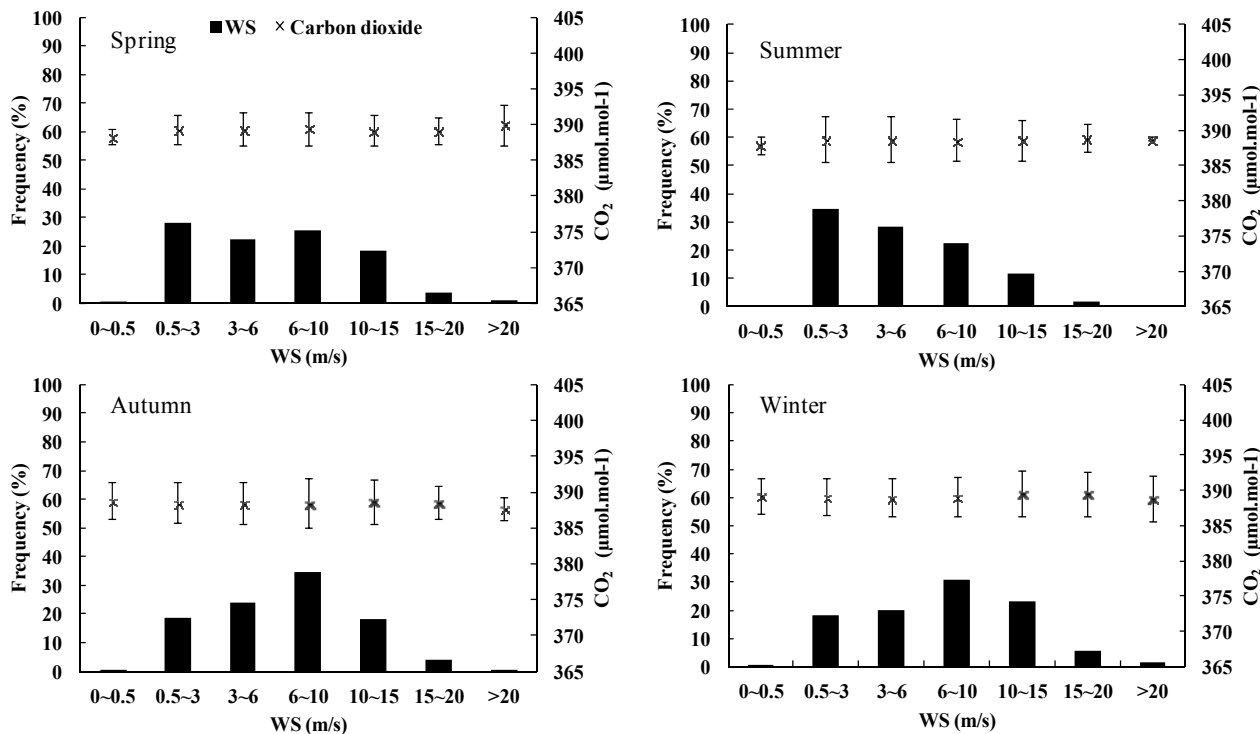


Figure 6. Frequency of occurrence of different wind speed scales and corresponding CO₂ mole fractions in four seasons at Zhongshan Station (2010 through 2013). The black bars stand for frequency of occurrence. The vertical bars stand for the amplitude of CO₂ mole fractions under the condition of same wind speed scale.



4. Background Characteristics of CO₂ Mole fractions and Seasonal Variation

Monthly averaged deviations of hourly mean CO₂ mole fractions from daily means at Zhongshan Station in January, April, July and October, representing four seasons respectively, are shown in Figure 7. It can be seen that the daily changes in four seasons are all quite small, and only subtle daily amplitude exists, which are 0.22 μmol·mol⁻¹, 0.19 μmol·mol⁻¹, 0.18 μmol·mol⁻¹ and 0.30 μmol·mol⁻¹, respectively. The results, therefore, suggest that there are no strong CO₂ sources and diurnal changes in the characteristics of the CO₂ sinks upwind of the station. This also indicates that the observation point on the east coast of Antarctica on a rocky outcropping without vegetation in summer and covered by snow in the other three seasons does not have a regional influence on the observations of background CO₂.

Figure 8 displays the average monthly CO₂ mole fraction month-by-month and the time sequence of minimum and maximum CO₂ values from 2010 through 2013 at Zhongshan Station. From this figure, the average monthly mole fraction changes exhibit a seasonal pattern as well as a steady increase in background CO₂ mole fractions. The amplitude of CO₂ mole fractions variability is higher in the austral summer. Similar phenomenon has been found at the Syowa and South Pole Stations, that is related to the large-scale transport of CO₂-depleted air masses to the Antarctic Continent [17]. From Figure 9, it can be seen that the seasonal variation of CO₂ mole fractions at Zhongshan reaches a minimum in March with a peak in November. As such, from Austral autumn through winter into spring (March–November), the cycle period for CO₂ mole fractions is largest while the CO₂ cycle in spring is noticeably slower

than that in autumn and winter. Summer (December–March) is the period when the mole fractions are the lowest.

Figure 7. Monthly averaged deviations of hourly mean CO₂ mole fractions from daily means at Zhongshan Station in January, April, July and October. The mole fraction is averaged over 2011–2012. Vertical bars represent the standard deviations.

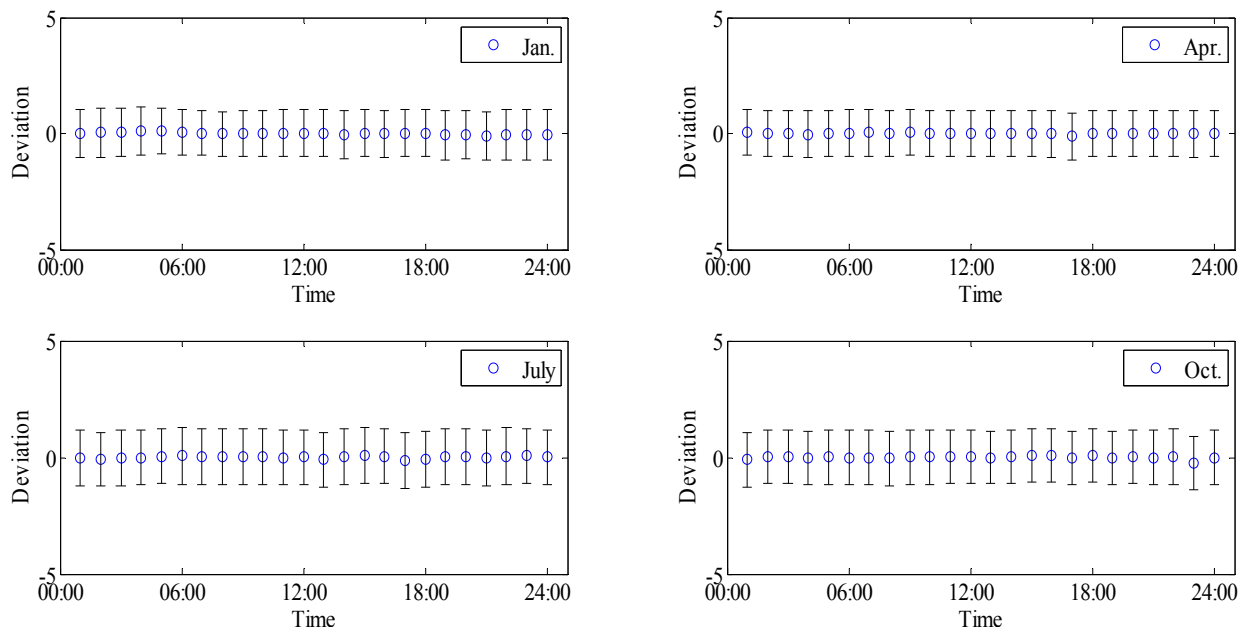
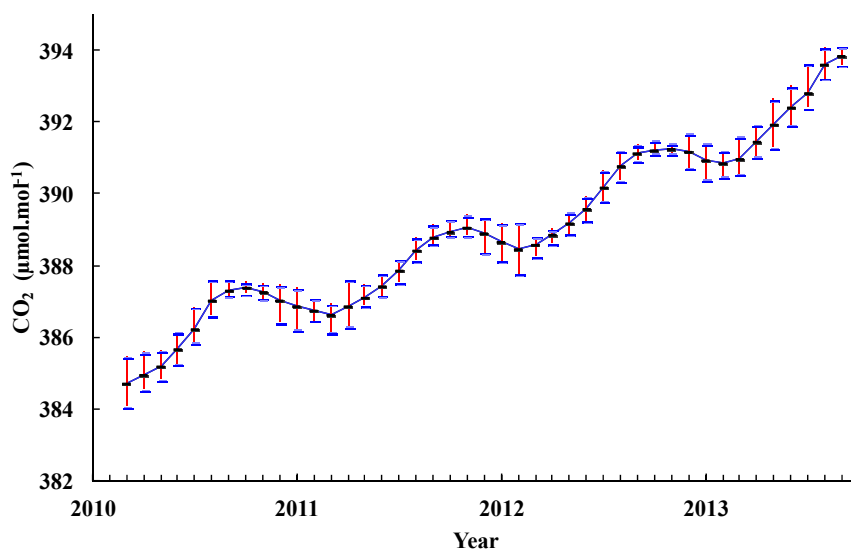


Figure 8. Average monthly CO₂ mole fraction at Zhongshan Station and the time sequence of its maximum and minimum values indicated by the red/blue lines (2010 through 2013). The vertical bars stand for the amplitude of CO₂ mole fractions variability of every month, which is higher in the austral summer.



In order to separate the long-term trend from the data set after processing, a digital filtering technique was applied to the daily mean CO₂ data to obtain the curve fit. Details of this fitting procedure have been presented by Nakazawa *et al.* [28]. Figure 9 shows the long-trend of the CO₂

mole fraction at Zhongshan Station from 2010 through 2013. It can be seen that the CO₂ mole fraction increased year by year from about 384 μmol·mol⁻¹ in 2010 to 393 μmol·mol⁻¹ in 2013.

Figure 9 shows the upward trend of CO₂ mole fraction during 2010 through 2013. To analyze the trend of CO₂ mole fraction in different seasons, Table 1 presents average mole fraction and increases in four seasons. In each season, the average mole fraction is increasing year-by-year; the increase in winter is the highest at 0.57% on average, followed by that in spring and autumn at 0.56%, and the rate in summer is the lowest at 0.50%. The data presented in Table 1 initially suggest that the mole fraction of CO₂ measured at Zhongshan Station is increasing annually at an accelerating rate.

Figure 9. Long-term trend (dotted line) of the CO₂ mole fraction at Zhongshan Station (2010 through 2013).

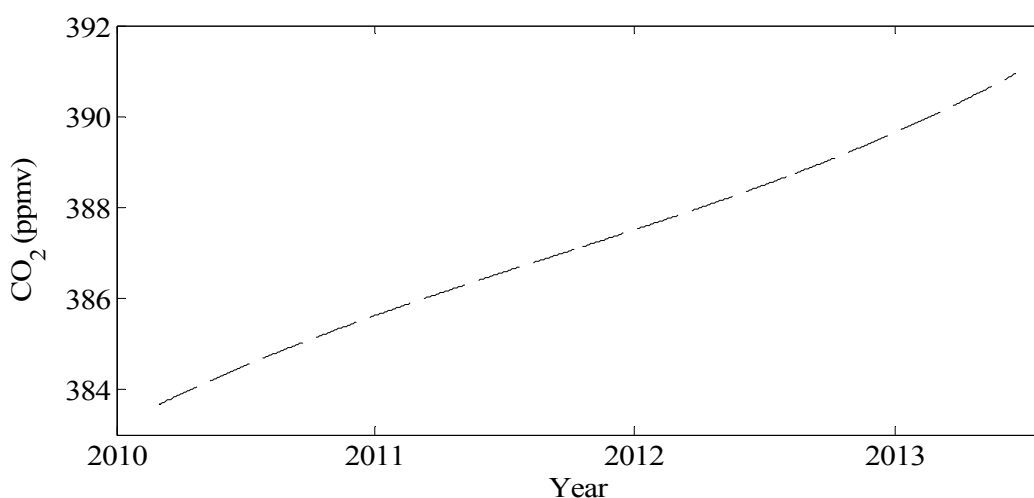


Table 1. Average CO₂ mole fraction (μmol·mol⁻¹; upper portion of the graph) and increase (lower portion of the graph) in four Seasons at Zhongshan Station.

Year	Spring	Summer	Autumn	Winter
2010	387.32	384.86	384.94	386.30
2011	388.93	386.56	386.86	387.90
2012	391.20	388.66	388.87	390.17
2013	393.87	390.99	391.45	392.95
2010–2011	0.42%	0.44%	0.50%	0.41%
2011–2012	0.58%	0.46%	0.52%	0.58%
2012–2013	0.68%	0.60%	0.66%	0.71%

In order to evaluate the representativeness of data observed on-line at Zhongshan Station, data of different stations from the World Data Centre for Greenhouse Gases (WDCGG) [29] have been compared as presented in Figure 10. The selected stations are Casey (66.28°S, 110.53°E), Syowa (69°S, 39.6°E), Palmer (64.92°S, 64°W), South Pole (90°S, 24.8°W) and Halley (75.6°S, 26.5°W). Their geographic locations are shown in Figure 1. Flask sampling and subsequent lab analysis are used to obtain the data for these five stations from 2010 through 2012. The monthly means derived from *in situ* measurements are more precise [30,31].

It can be seen from Figure 10 that CO₂ mole fractions observed at Zhongshan Station are quite similar to those measured at other stations around Antarctica; station records show similar ranges, all falling between 384 and 392 μmol·mol⁻¹. The peak of CO₂ mole fraction is at Casey Station (391.7 μmol·mol⁻¹) and the maximum at Zhongshan Station is 391.3 μmol·mol⁻¹ while the lowest value occurs at Halley Station (384.5 μmol·mol⁻¹) and the minimum at Zhongshan Station is 384.7 μmol·mol⁻¹. Table 2 shows that the difference in average annual CO₂ mole fraction between each station is less than 1 μmol·mol⁻¹, and the interannual variation of all stations presents a clear upward trend of 1.5–2.2 μmol·mol⁻¹·yr⁻¹, indicating that there is little difference in spatial distribution of CO₂ mole fractions in the Antarctic area. The average annual mole fraction and increase of CO₂ at Zhongshan Station are close to those at other stations, suggesting that CO₂ data at this station is representative of the background characteristics of atmospheric composition in Antarctica.

Figure 10. Time sequence of average monthly CO₂ mole fraction at each CO₂ monitoring station in Antarctica.

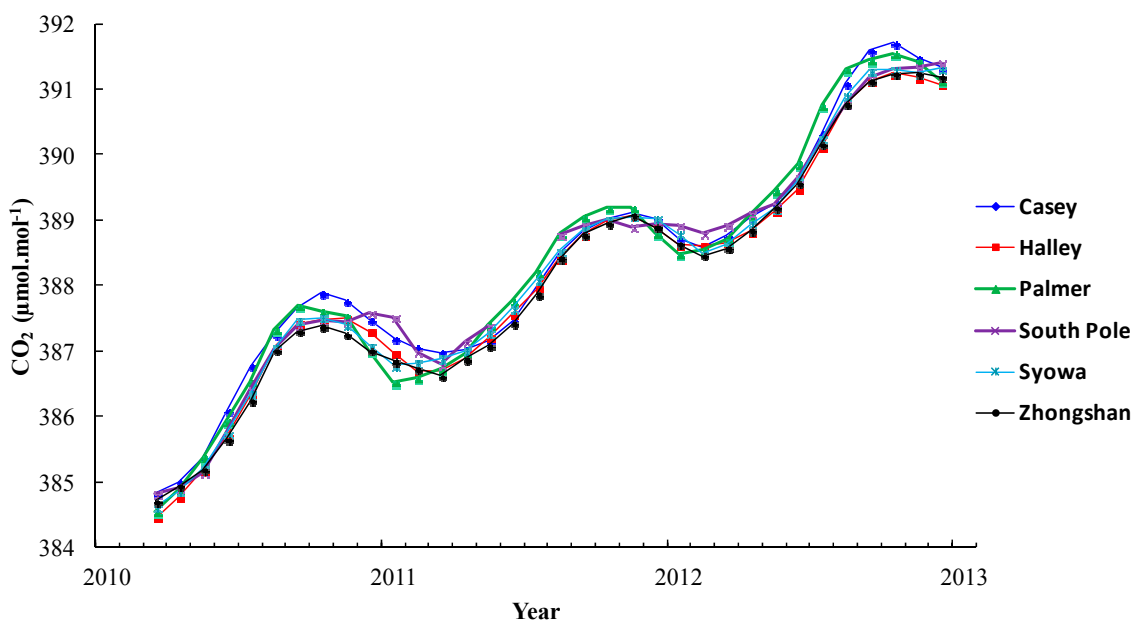


Table 2. Average annual CO₂ mole fraction (μmol·mol⁻¹; upper) and its increase at each station (lower).

Year	Casey	Palmer	South Pole	Halley	Syowa	Zhongshan
2010	386.61	386.44	386.40	386.31	386.33	386.27
2011	387.95	387.94	388.04	387.95	387.92	387.80
2012	390.14	390.14	390.08	390.12	389.99	389.92
2010–2011	1.54 (0.40%)	1.50 (0.39%)	1.64 (0.42%)	1.64 (0.40%)	1.59 (0.41%)	1.53 (0.40%)
2011–2012	2.19 (0.56%)	2.20 (0.57%)	2.04 (0.53%)	2.17 (0.53%)	2.07 (0.54%)	2.12 (0.55%)

5. Summary and Conclusions

The mole fraction of CO₂ observed at Zhongshan Station is only slightly affected by wind direction and speed. Local pollution from the station under westerly and calm winds accounted for only 1.7% of the total measurement period. Once this contamination is removed from the data set, the CO₂ observations

can be used to represent the background mole fraction of CO₂ measured on the east coast of the Antarctic continent.

The average daily range of CO₂ mole fraction in all four seasons is small: 0.22 μmol·mol⁻¹ (January), 0.19 μmol·mol⁻¹ (April), 0.18 μmol·mol⁻¹ (July) and 0.30 μmol·mol⁻¹ (October) respectively. The seasonal variation of CO₂ mole fraction at Zhongshan Station reaches the minimum in March after which it begins to rise constantly to the peak in November.

The monthly mean CO₂ mole fraction measured at Zhongshan station is similar to that of other stations in Antarctica, and their annual amplitudes are all within the range of 384–392 μmol·mol⁻¹ during the period 2010–2013. The annual increase in recent years is about 2 μmol·mol⁻¹·yr⁻¹. There is no significant difference in the mole fractions of CO₂ measured around the coast of the Antarctic continent showing that the CO₂ observed in Antarctica has been fully mixed in the atmosphere and has not been greatly affected by local environments once obvious pollution from station activities is removed. Many of the Antarctic CO₂ measurement records are from flask samples taken at intervals of a week or longer. The continuous CO₂ measurements at Zhongshan station will be maintained for the foreseeable future and compared to data from other Antarctic stations to ensure the Zhongshan measurements maintain their accuracy and consistency. The continuous data will also be used to study possible scientific benefits of continuous CO₂ measurements compared to flask data and possible measurement of CO₂ uptake by biological processes in the high primary production Antarctic waters.

Acknowledgments

This work was supported by the Program of China Polar Environment Investigation and Assessment (Project No. CHINARE2011–2015), the authors appreciate the assistance of all staff wintered in Zhongshan station during the data collection.

Author Contributions

Lingen Bian supervised the research. Jie Tang and Chang Lu were involved in the data analysis. Russell. C. Schnell corrected mistakes and edited the paper. All of authors contributed to the discussion of the results. Yulong Sun and Lingen Bian wrote the manuscript.

Conflicts of Interest

The authors declare no conflict of interest.

References

1. Climate Change 2013: The Physical Science Basis. Working Group I Contribution to the IPCC Fifth Assessment Report. Available online: <http://www.climatechange2013.org/> (accessed on 18 September 2014).
2. Ramanathan, V.; Cicerone, R.J.; Singh, H.B.; Kiehl, J.T. Trace gas trends and their potential role in climate change. *J. Geophys. Res.: Atmos.* **1985**, *90*, 5547–5566.
3. Rastogi, M.; Singly, S.; Pathak, H. Emission of carbon dioxide from soil. *Curr. Sci.* **2002**, *82*, 510–517.

4. Maccougall, A.H.; Eby, M.; Weaver, A.J. If anthropogenic CO₂ emissions cease, will atmospheric CO₂ concentration continue to increase? *J. Clim.* **2013**, *26*, 9563–9576.
5. Wang, W.C.; Yung, Y.L.; Lacis, A.A.; Mo, T.; Hansen, J.E. Greenhouse effects due to man-made perturbations of trace gases. *Science* **1976**, *194*, 685–690.
6. Joshua, S. Global change: Nice, microbes and methane. *Nature* **2000**, *403*, 375–377.
7. WMO. *Greenhouse Gas Bulletin: The State of Greenhouse Gases in the Atmosphere Using Global Observations through 2012*; WMO: Geneva, Switzerland, 2013.
8. Houghton, R.A. Revised estimates of the annual net flux of carbon to the atmosphere from changes in land use and land management 1850–2000. *Tellus B* **2003**, *55*, 378–390.
9. Andreae, M.O.; Merlet, P. Emission of trace gases and aerosols from biomass burning. *Glob. Biogeochem. Cycles* **2001**, *15*, 955–966.
10. Caillon, N.; Severinghaus, J.P.; Jouzel, J.; Barnola, J.; Kang, J.; Lipenkov, V.Y. Timing of atmospheric CO₂ and Antarctic temperature changes across Termination III. *Science* **2003**, *299*, 1728–1731.
11. Zhou, L.X.; Zhou, X.J.; Zhang, X.C.; Wen, Y.P.; Yan, P. Progress in the study of background greenhouse gases at Waliguan observatory. *Acta Meteorol. Sin.* **2007**, *65*, 458–468. (in Chinese)
12. Agee, E.; Orton, A.; Rogers, J. CO₂ snow deposition in Antarctica to curtail anthropogenic global warming. *J. Appl. Meteorol. Climatol.* **2013**, *52*, 281–288.
13. WMO. *Strategy for the Implementation of the Global Atmosphere Watch Programme (2001–2007), a Contribution to the Implementation of the WMO Long-Term Plan*; GAW NO.142; WMO: Geneva, Switzerland, 2001.
14. Komhyr, W.D.; Gammon, R.H.; Harris, T.B.; Waterman, L.S.; Conway, T.J.; Taylor, W.R.; Thoning, K.W. Global atmospheric CO₂ distribution and variations from 1968–1982 NOAA/GMCC CO₂ flask sample data. *J. Geophys. Res.* **1985**, *90*, 5567–5596.
15. Lai, X. *Analysis of the Background Concentrations of Atmospheric Composition in Polar Regions*; Academy of Meteorological Sciences: Beijing, China, 2012
16. Keeling, C.D.; Adams, J.A.J.; Ekdahl, C.A.J.; Guenther, P.R. Atmospheric carbon dioxide variations at the South Pole. *Tellus* **1976**, *28*, 552–564.
17. Atmospheric Carbon Dioxide Record from the South Pole. Available online: <http://cdiac.ornl.gov/trends/co2/sio-spl.html> (accessed on 22 September 2014)
18. Morimoto, S.; Nakazawa, T.; Aoki, S.; Hashide, G.; Yamanouchi, T. Concentration variations of atmospheric CO₂ observed at Syowa Station, Antarctica from 1984 to 2000. *Tellus B* **2003**, *55*, 170–177.
19. Ghude, S.D.; Jain, S.L.; Arya, B.C. Temporal evolution of measured climate forcing agents at South Pole, Antarctica. *Curr. Sci.* **2009**, *96*, 49–57.
20. Wang, Y.T.; Bian, L.G.; Ma, Y.F.; Tang, J.; Zhang, D.Q.; Zheng, X.D. Surface ozone monitoring and background characteristics at Zhongshan Station over Antarctica. *Chin. Sci. Bull.* **2011**, *56*, 1011–1019.
21. Crosson, E.R. A cavity ring-down analyzer for measuring atmospheric levels of methane, carbon dioxide, and water vapor. *Appl. Phys. B* **2008**, *92*, 403–408.

22. Fang, S.X.; Zhou, L.X.; Zang, K.P.; Wang, W.; Xu, L.; Zhang, F.; Yao, B.; Liu, L.X.; Wen, M. Measurement of atmospheric CO₂ mixing ratio by cavity ring-down spectroscopy (CRDS) at the 4 background stations in China. *Acta Sci. Circumst.* **2011**, *31*, 624–629. (in Chinese)
23. Anna, K.; Colm, S.; Pieter, T.; Timothy, N. AirCore: An innovative atmospheric sampling system. *J. Atmos. Ocean. Technol.* **2010**, *27*, 1839–1853.
24. Chen, H.; Winderlich, J.; Gerbig, C. High-accuracy continuous airborne measurements of greenhouse gases (CO₂ and CH₄) using the cavity ring-down spectroscopy (CRDS) technique. *Atmos. Meas. Tech.* **2010**, *3*, 375–386.
25. Rella, C. *Accurate Greenhouse Gas Measurements in Humid Gas Streams Using the Picarro G1301 Carbon Dioxide/Methane/Water Vapor Gas Analyzer*; White Paper; Picarro Inc.: Sunnyvale, CA, USA, 2010.
26. Zhou, L.X.; Wen, Y.P.; Li, J.L.; Tang, J.; Zhang, X.C. Impact of local surface winds on atmospheric methane background concentration at Mt.Waliguan. *J. Appl. Meteorol. Sci.* **2004**, *15*, 257–265. (in Chinese)
27. Zhou, L.X.; Tang, J.; Wen, Y.P.; Zhang, X.C. Impact of local surface wind on atmospheric carbon dioxide background concentration at Mt.Waliguan. *Acta Sci. Circumst.* **2002**, *22*, 135–139. (in Chinese)
28. Nakazawa, T.; Ishizawa, M.; Higuchi, K.A.Z. Two curve fitting methods applied to CO₂ flask data. *Environmetrics* **1997**, *8*, 197–218.
29. Global Atmosphere Watch. Available online: <http://ds.data.jma.go.jp/gmd/wdcgg/cgi-bin/wdcgg/catalogue.cgi> (accessed on 22 September 2014).
30. Tans, P.P.; Thoning, K.W.; Elliott, W.P.; Conway, T.J. Error estimates of background atmospheric CO₂ patterns from weekly flask samples. *J. Geophys. Res.: Atmos.* **1990**, *95*, 14063–14070.
31. Komhyr, W.D.; Waterman, L.S.; Taylor, W.R. Semiautomatic nondispersive infrared analyzer apparatus for CO₂ air sample analyses. *J. Geophys. Res.: Atmos.* **1983**, *88*, 1315–1322.

© 2014 by the authors; licensee MDPI, Basel, Switzerland. This article is an open access article distributed under the terms and conditions of the Creative Commons Attribution license (<http://creativecommons.org/licenses/by/4.0/>).